6th International Meeting
on
Wind Turbine Noise
Glasgow 20-23 April 2015

Aeroacoustic wind tunnel experiment for serration design optimisation and its application to a wind turbine rotor

J. Hurault Vestas Technology UK Ltd, Stag Lane, Newport, Isle of Wight, PO30 5TR, UK E-mail: jehur@vestas.com

A. Gupta Vestas America, Houston, Texas, USA E-mail: angpt@vestas.com

E. Sloth Vestas Wind Systems A/S, Hedeager 42, Aarhus, 8200, DK E-mail: erslo@vestas.com

N. C. Nielsen Vestas Wind Systems A/S, Hedeager 42, Aarhus, 8200, DK E-mail: ncn@vestas.com

A. Borgoltz Virginia Tech, Aerospace & Ocean Enginering Dept., 660 McBryde Hall, 225 Stranger Street, Blacksburg, VA, 24061, USA E-mail: aborgolt@vt.edu

P. Ravetta AVEC Inc., 3154 State Street, Suite 2230, Blacksburg, VA 24060, USA E-mail: pravetta@avec-engineering.com

1. Summary

In order to reduce wind turbine noise at the source, serrations have been designed and fitted to a 3 MW horizontal axis wind turbine (HAWT). It has been demonstrated by numerous authors that the turbulent boundary layer trailing edge (TBL-TE) noise generated in the last third of the blade span is responsible for most acoustic energy emitted by modern pitch regulated megawatt class HAWT. Serrations are specifically targeting TBL-TE noise reduction.

This paper describes the serrations experimental design optimization performed at the Virginia Tech Stability Wind Tunnel in its aeroacoustic configuration. The Virginia Tech wind tunnel is a closed section wind tunnel equipped with an anechoic test section and a microphone array to localize noise sources. The airfoil and wind tunnel operating conditions are representative of the full scale operating conditions of a blade tip section. Twenty serration configurations have been tested in the wind tunnel and are designed for low impact on aerodynamic loads and higher noise reduction.

The optimum values for each geometry parameter have been identified, and then serrations have been designed for a full scale blade. IEC 61400-11 ed.3 acoustic tests have been performed on the field and it has been found that these serrations reduced the overall A-weighted sound power by 2-3 dBA depending on wind speed. Analysis of the one third octave spectrum shows noise reduction for a wide frequency range, without high frequency noise increase as reported by some authors for different serration designs.

2. Introduction

Howe [1][2] discussed the production of sound by low Mach number turbulent flow over the trailing edge of a serrated airfoil (semi-2D) at zero AOA. The simplified analytical treatment in these papers and his textbook still remain effective guides to understand the primary mechanisms of noise reduction and design drivers. For serrations of spanwise wavelength λ, amplitude h, and at radian frequencies f satisfying $fh/U>>1$ (U being the main stream velocity), trailing edge noise is reduced relative to that for a straight edge by $10\log(10h/\lambda)$.

Researchers at National Aerospace Laboratory (NLR) in the JOULE III project "Investigation of Serrated Trailing Edge Noise (STENO)" investigated the application of STE to reduce the TBL-TE noise of wind turbine blades by wind tunnel tests, numerical prediction methods and free field measurements [3][4][5]. Wind tunnel measurements using 2D airfoil sections showed that the STE reduced the level of TBL-TE noise significantly. However, strong indications were found that the noise reduction mechanism may be less effective in case of strong 3D flow (e.g. tip region) and the existence of perpendicular pressure gradient across the serrations. The work described led to the conclusion that it is worthwhile to investigate the optimal application of STE for real wind turbines.

In the STENO project [4] a reduction in the total noise level of about 2 dB in the free-field experiments for the range of operational incidence angles using the STE on the UNIWEX turbine was found. The reduction is much less than the theory, numerical calculations and wind tunnel tests predicted. They could not explain this behaviour, but they provided 2 possible effects that could play a certain role: first, the alignment of the serrations; second, the boundary layer influence caused by serrations. The pressure jump perpendicular to the serrations can cause additional small scale turbulence due to flow separation on the serration's suction side. This can cause the increase of the high frequency noise. The pressure jump also affects the large scale fluctuations inside the boundary layer of the suction side of the airfoil and increase the low frequency noise. It is also shown in the STENO report that the serration cross section profile shape has a strong impact on both airfoil aeroacoustic and aerodynamic performance.

Researchers from NLR, Energy Research Centre of the Netherlands (ECN) and Institute of Aerodynamics and Gas Dynamics (IAG) at University of Stuttgart tried to reduce TBL-TE noise by modifying the airfoil shape and/or implementing STE, during the European project Design and Testing of Acoustically Optimized Airfoils for Wind Turbines (DATA) [6]. They did the validation test on a scaled wind turbine model with a two-bladed 4.5 m diameter rotor in the open jet test section of DNW-LLF with the 9.5 m x 9.5 m nozzle. Measurements were performed for one baseline and two acoustically optimized rotors. The tests were conducted with a 136 microphone acoustic array. The optimized airfoil shapes showed 2-4 dB TBL-TE noise reduction when compared to the baseline model, without loss in power production. A further reduction of 2 dB can be achieved by the application of STE.

In the SIROCCO project [7], acoustic field measurements on a 94 m diameter, three-bladed wind turbine has been conducted. One standard blade, one blade with acoustically optimized airfoil shape, and one standard blade with STE were fitted on a HAWT. Test results for the baseline blade showed that the dominant source was TBL-TE noise from the outer 25% of the blade. Both optimized blades showed a significant TBL-TE noise reduction at low frequencies. For clean blade at normal operation conditions, average overall noise reduction of 0.5 dB for the blade with optimized airfoil shape and 3.2 dB for the blade with STE were observed. For both blades, the noise reduction increased with increasing wind speed on the pitch-regulated test turbine.

Sandberg and Jones [8] did Direct Numerical Simulations (DNS) for NACA0012 airfoil self-noise at low Reynolds number ($Re\sim5\times10^4$), with and without STE. The one-third octave averaged contours show that TBL-TE noise is reduced at high frequencies while no significant difference is observed at low frequencies. This might be related to the acoustic feedback loop

occurring at a frequency below the threshold frequency for which STE are effective, or because the laminar-turbulent transition is dominated by a three-dimensional instability mechanism which is unaffected by the STE.

Herr and Reichenberger [9] presented their results on innovative trailing edge design, as part of the EC co-financed project OPENAIR. They did serial tests for different designs, such as porous materials, serrations, slotted trailing edges and brushes, at DLR's Acoustic Wind-Tunnel Braunschweig (AWB). It was found that trailing edges with brushes have the best noise reduction, almost 10 dB in a certain frequency range. Although this indicates significant potential for noise reduction, the technology is not as mature as STE and has some significant issues with material wear and lifetime effectiveness. Porous, serrated and slotted trailing edges can achieve a noise reduction of up to 4 dB, depending on the configuration. Pressure distribution measurements reveal a small influence on the airfoil's suction peak for all trailing edge modifications.

Gruber et al. [10] also did an experimental investigation of the mechanisms involved in airfoil TBL-TE noise reduction and noise increase observed by the implementation of sawtooth serrations at the trailing edge. The paper presents the results of an experimental campaign during which a set of over 30 sawtooth geometries were tested for noise on a NACA6512 airfoil. It is shown that the frequency above which noise is increased is dictated by the boundary layer Strouhal number. Hot wire velocity measurements and flow visualization reveal that these noise sources are located between the sawtooth of the STE, verifying the fundamentals of the Howe theory.

The use of serrated trailing edges for wind turbine noise reduction has now become a mature technology with several academic/research institutions and wind turbine manufacturers demonstrating its effectiveness in wind tunnel and turbine tests leading to commercial products. However, to the knowledge of the authors, no study has been published regarding high Reynolds number wind tunnel testing (Re > 3 millions), representative of wind turbine applications. The work described in this document aimed to develop noise-reduction serrations, and the design capability and technology database to apply them to Vestas rotors. As it can be seen in section 4 of the present paper, 2-3 dBA (OASPL) noise reduction has been validated for a contemporary Vestas rotor like the V117 3.3MW.

3. Wind tunnel experimental campaign

3.1. Aeroacoustic wind tunnel specifications

All tests were performed in the Virginia Tech Stability Wind Tunnel. This facility is a continuous, single return, subsonic wind tunnel with 7.3-m long removable rectangular test sections of square cross section 1.85m on edge. The general layout is illustrated in Figure 1. The tunnel is powered by a 0.45-MW variable speed DC motor driving a 4.3-m propeller at up to 600 RPM. This provides a maximum speed in the test section (with no blockage) of about 80m/s and a Reynolds number per meter up to about 5,000,000. Temperature stabilization is obtained through an air exchange tower open to the atmosphere and located downstream of the fan. Downstream of the tower the flow is directed into a 5.5×5.5m settling chamber containing 7 turbulence-reducing screens each with an open area ratio of 0.6 and separated by 0.15m. Flow exits this chamber through the 9:1 contraction nozzle which further reduces turbulence levels and accelerates the flow to test speed as it enters the test section.

Acoustic treatment of the flow path includes a 25-mm thick melamine foam liner used to treat the side walls and ceiling of the diffuser (section 1 in figure 1), a 50-mm thick melamine and urethane foam liner on the walls and ceiling of the south leg of the tunnel (section 2) and a

50mm urethane foam liner on the side walls and floor of the north leg of the tunnel (section 3) and on the side walls of the portion of the settling chamber upstream of the screens (section 4).

Flow through the empty test section (measured with a hard-wall test section in place) is both closely uniform and of very low turbulence intensity. Turbulence levels are as low 0.016% at 12m/s and increase gradually with flow speed reaching 0.031% at 57m/s. Choi and Simpson [11] measured the lateral integral scales of the streamwise velocity in both the horizontal Lz and vertical Ly directions. They found Lz=56mm for 15m/s and 28mm for 37.5m/s and Ly=122mm for 15m/s and 25mm for 37.5m/s.

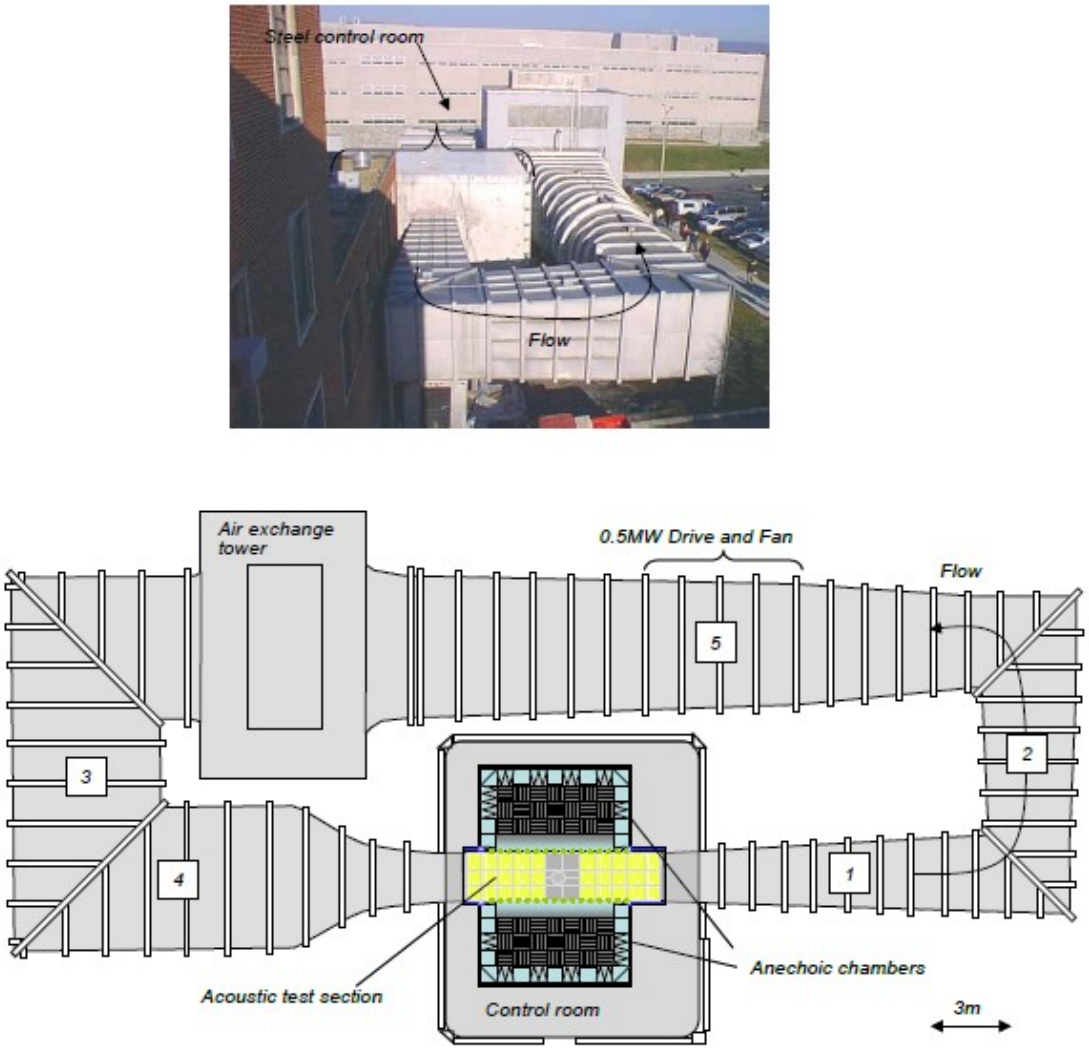

Figure 1: Picture and schematic of VT Stability Wind Tunnel.

The Virginia Tech Stability Wind Tunnel has a novel Kevlar-walled anechoic test section that allows sound out into the surrounding anechoic chambers, but contains the flow (figures 2 and 3). As a consequence, high fidelity acoustic measurements can be made under aerodynamic conditions that very closely mimic free flight. The anechoic system consists of an acoustic test section flanked by two anechoic chambers (figures 1 and 3). Large rectangular openings in the side walls which extend 4.2m in the streamwise direction and cover the full 1.83-m height of the test section serve as acoustic windows. Sound generated in the test flow exits the test section through these into the anechoic chambers to either side. Large tensioned panels of Kevlar cloth cover these openings permitting the sound to pass while containing the bulk of the flow. This use of the material was pioneered by Jaeger et al. [12]. They were investigating different means of shielding a phased array microphone system embedded in the wall of a test section. They found this cloth to transmit sound with very little attenuation up to at least 25kHz. The Stability Tunnel is the first anechoic wind tunnel to employ this technology on a facility scale.

The test section arrangement thus simulates a half-open jet, acoustically speaking. The Kevlar windows eliminate the need for a jet catcher and, by containing the flow, substantially reduce the lift interference when airfoil models are placed in the test flow. The floor and ceiling of the test-section are made of Kevlar covered perforated aluminum panels. The volume behind the panels' surface is filled with 0.457m-high foam wedges that eliminate acoustic reflections at frequencies above 190Hz (figure 3).

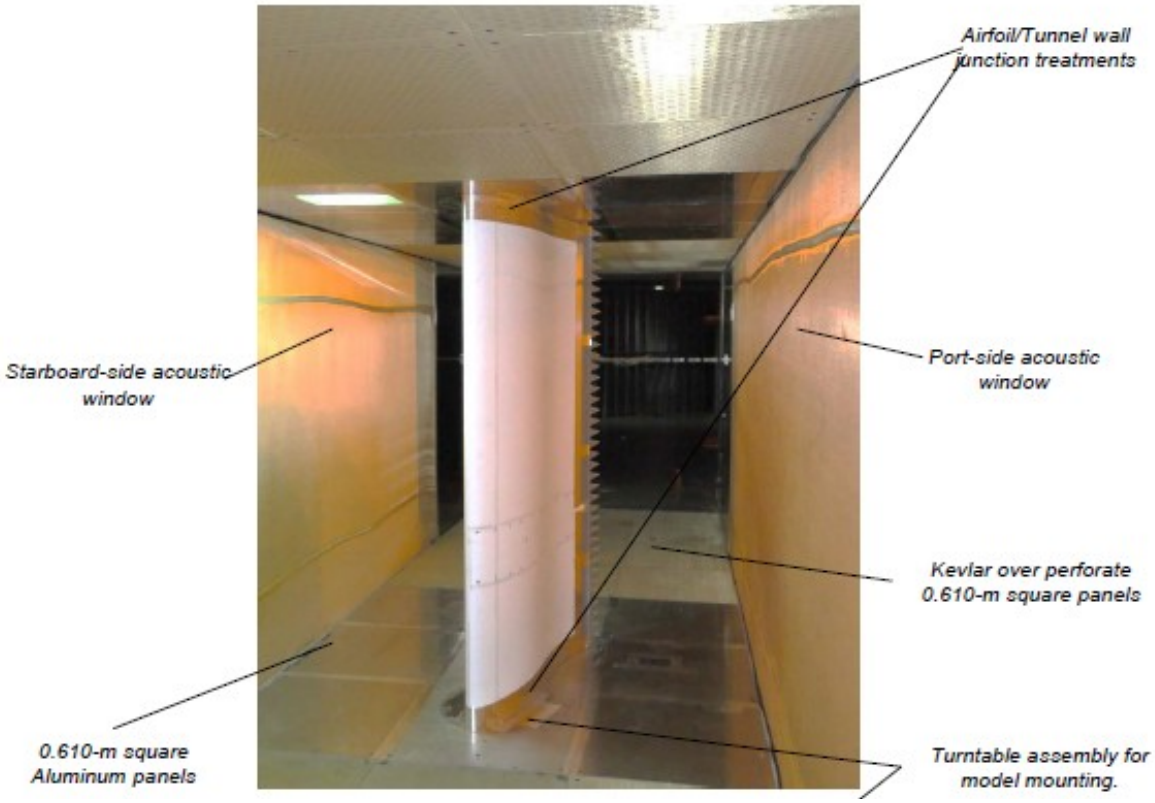

Figure 2: Test section with Kevlar wall acoustic windows and airfoil model fitted with serrations.

The Risø B1 airfoil model was initially studied as part of a program sponsored by NREL [13]. The geometry was developed by the Risø National Laboratory (figure 2). The model is designed to have a 1.8m span, an overall airfoil chord of 914mm and a relative thickness of 18%. The model is made of a fiberglass skin and a fill of fiberboard and polyurethane foam. The model is instrumented with approximately 80 pressure taps of 0.5 mm internal diameter located near the mid-span. The nominal chordwise locations of the pressure taps are the same on both sides of the airfoil.

3.2. Aerodynamic measurement uncertainties

Uncertainty in the setting of absolute angle of attack is estimated as ±0.15 degrees based principally on a cautious interpretation of first hand experiences working with the models and the slew drive system. The principle source of this is the accuracy of the initial alignment of the airfoil. The uncertainty in angle of attack changes in any one run is therefore considerably smaller and likely 0.1 degrees.

Uncertainty in pressure, lift and moment coefficients are estimated at ±0.007, ±0.012 and ±0.0014 respectively, these being generally very small fractions of the measured values. Uncertainty in drag coefficient is estimated at 5% of the measured value.

3.3. Microphone phased array processing

The microphone phased array used in this effort consisted of a 117-channel, 1.1 m diameter planar array, with microphones being arranged in a 9-armed spiral of 13 microphones. A picture of the set-up and a schematic showing the position of the 117-channel array is shown in figure 3. The microphones used in this array are Panasonic model WM-64PNT Electret microphones. These microphones have a flat frequency response from 20-16,000 Hz and a sensitivity of -44 +/- 3 dB Re 1V/Pa at 1 kHz. All microphones used in the array were calibrated before being installed in the array and selected to be within ±5° phase and ±0.4 dB amplitude from 500 Hz to 16,000 Hz.

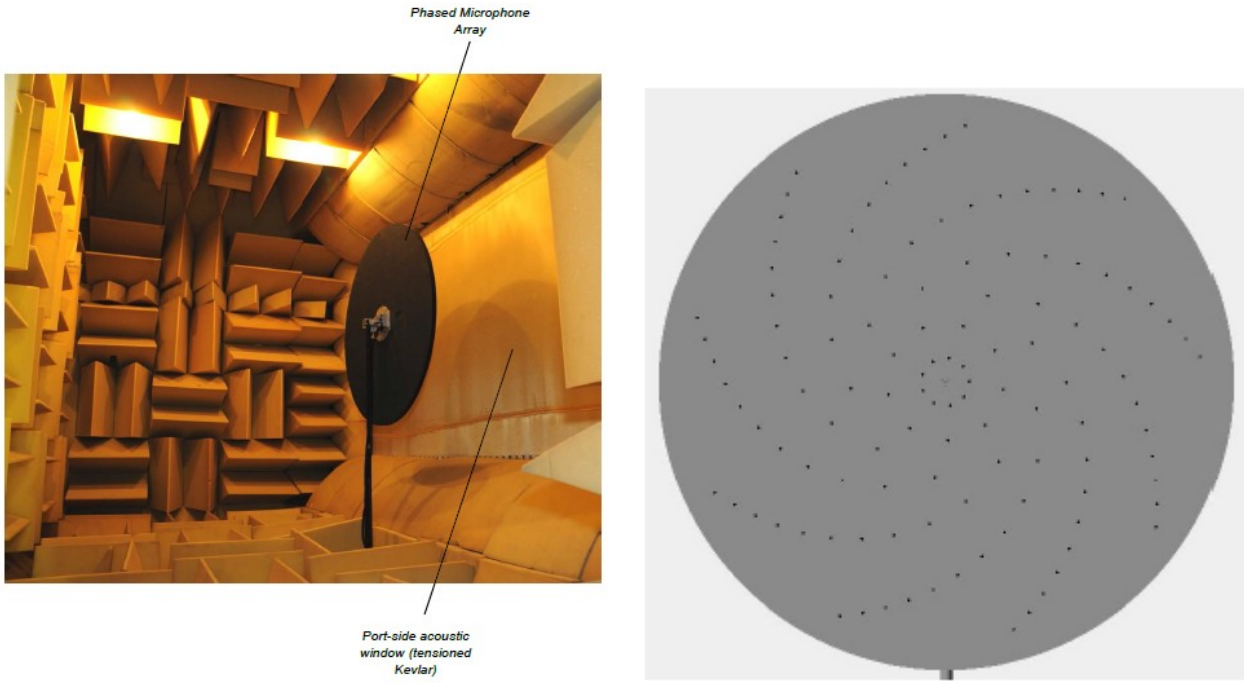

Figure 3: Phased microphone array in the wind tunnel semi-anechoic chamber (left) and microphone layout (right).

A 128-channel, high speed data acquisition system was used in this test. This system supports simultaneous sampling from all 128 channels at up to 200 KS/s. The microphone signals were fed into an AVEC-designed signal conditioning and filtering box, which provided power to the microphones as well as anti-aliasing filtering at 20 kHz (corner frequency). The conditioned signals were then fed to a computer with two 64-channel PCI-based data acquisition cards set up for simultaneous sampling. For this test, data was acquired during 32 seconds at a sampling rate of 51,200 Hz.

The software used to acquire, process and analyze the data was previously developed by AVEC. The software allows processing the test data using conventional beamforming as well as beamforming with flow, i.e. to account for refraction in the boundary layer. The beamforming results can also be post-processed using a proprietary technique developed by AVEC to remove contaminating noise sources.

The raw data was converted to the frequency domain and the cross-spectral matrices were averaged using 200 blocks of 8192 samples (i.e. 32 seconds of data). The frequency domain beamforming was conducted in 1/12th octave bands. Diagonal removal was applied to reduce the effects of uncorrelated noise. For the results in this work, the “allowed” area was defined as shown in figure 4. The integrated spectra were computed over a region covering the center one third of the trailing edge in the span-wise direction. This allowed for a more accurate estimation of the trailing edge noise by avoiding other spurious sources.

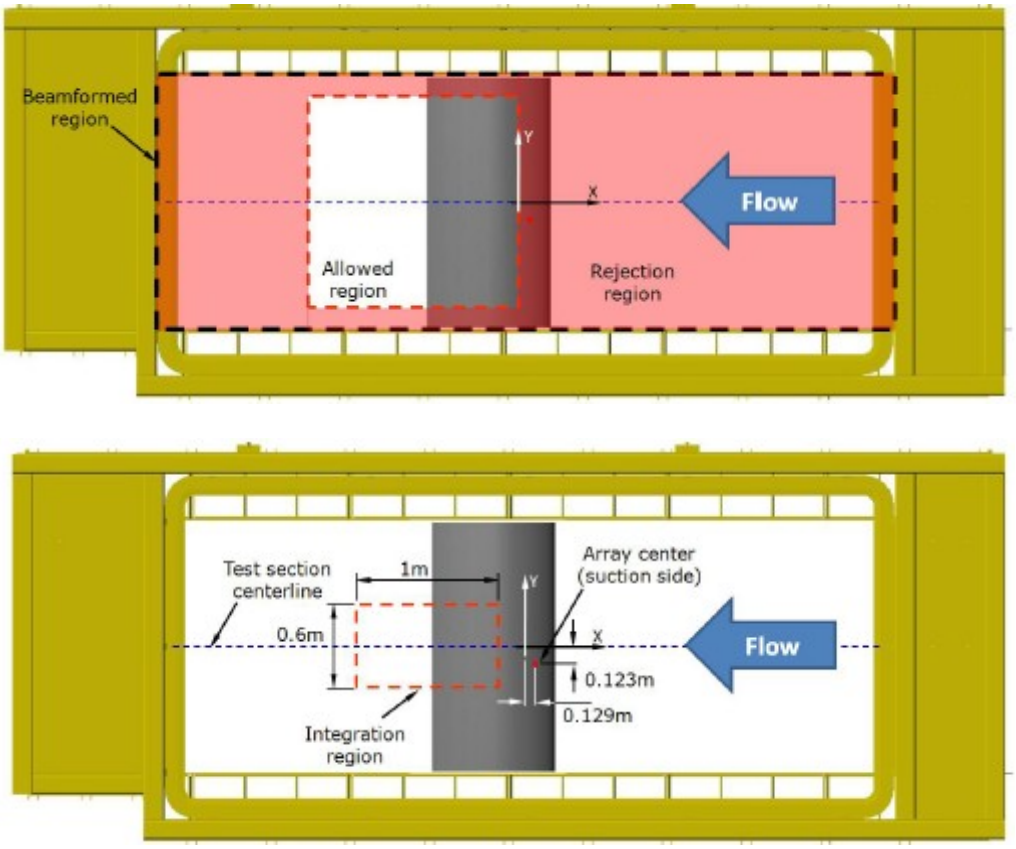

Figure 4: Set-up of the beamforming processing, with rejection region (top) and integration region for overall sound level and octave spectra (bottom).

In the Z-direction, only the plane Z=0 was used in the integration. A few test cases were integrated using a region from Z=-0.18m to Z=0m and, as expected, it was found that the integrated levels vary insignificantly when using a 3D grid. Therefore, it was decided to only use the Z=0 plane, significantly reducing data processing and analysis time. The reason for the very good agreement between 2D and 3D results is the inherently low resolution of the array in the direction normal to it (the Z-axis) [14].

The noise transmission losses due to the Kevlar windows and the boundary layers are corrected during the post-processing. The detailed description of the correction could be found in reference [15]. This correction was applied to all the integrated spectra results presented and also the overall noise level. However, this correction was not applied to the levels shown in the acoustic maps.

Since the tests were conducted at constant Reynolds number (instead of constant flow speed), corrections for flow speed and Strouhal number had to be applied to each configuration. These corrections account for the differences in noise level and frequency. The first step in this process involves determining the scaling law for noise levels as a function of free-stream velocity. To determine the scaling law, the results obtained at different Reynolds numbers were used. The analysis was conducted using the Strouhal number. Typically, Strouhal scaling is based on boundary layer thickness. However, since such data is not available, the airfoil chord was used as the characteristic length, this is:

$$\mathrm{St} = \frac{\mathrm{f} * \mathrm{c}}{U}$$

Where St is the Strouhal number,
f (Hz) is the frequency of interest,
c (m) is the chord of the airfoil, and
U (m/s) is the free-stream velocity.

The results show that the baseline TBL-TE noise levels scale well with the 5th power of the free stream velocity, consistent with the theory developed by Ffowcs-Williams and Hall [16]. The next step consists of choosing a single flow speed at which all the configurations will be compared (56 m/s was selected as it approximates the mean flow speed during the tests). This allows accurately comparing the noise spectra for different configurations. The levels are then corrected by the 5th power of the ratio of free stream velocities using:

$$SPL_{corr} = SPL_{test} + 10 * log\left(\frac{U_{corr}}{U_{test}}\right)^5$$

Where U_{corr} is the target flow speed to which results are extrapolated,
U_{test} is the free-stream velocity during the test,
SPL_{test} is the SPL obtained from the test data,

The frequencies are then scaled with respect to the chord-based Strouhal number. Since all the cases to be compared have the same chord, the corrected frequency is scaled only by the ratio of flow speeds as:

$$f_{corr} = f_{test}\frac{U_{corr}}{U_{test}}$$

Where f_{corr} is the Strouhal number-corrected frequency, and
f_{test} is the actual frequency from the test data.

3.4. Experimental test matrix

The present study provides an assessment on the effects of various parameters of the serration geometry (figure 5) on the lift, drag and noise of a wind turbine airfoil model. From the literature review, the triangular STE has been highlighted as giving the best noise reduction, and the critical STE geometrical parameters include: STE length to chord ratio (h), aspect-ratio (SAR), angle of STE to the chord (ASTE). The serration length h varied from 5 to 20% chord. Associated aspect-ratios were investigated between 2 and 8, with several root radii.

A total of 21 configurations have been tested during this study. These configurations required a total of 14 different serrated extensions (examples on figure 5). All the serrations, made of three different materials, were smooth and with very low roughness. The serration extensions were mounted on the pressure side of the airfoil. The STE have been designed and allied with care to ensure a smooth transition with the airfoil geometry.

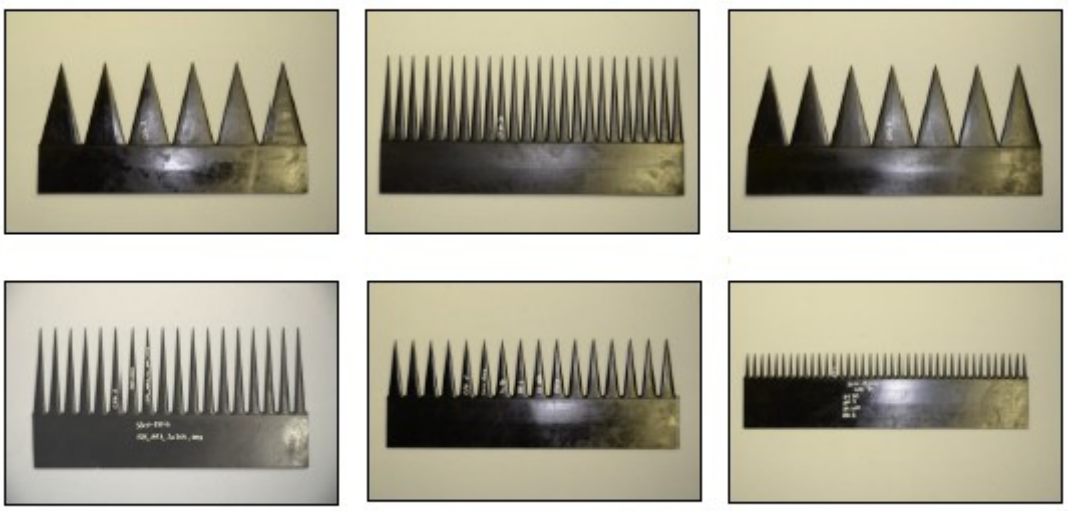

Figure 5: Picture of a few STE tested during this measurement campaign.

Measurements were made at a range of Reynolds number based on the chord between 1.6 and 3.2 million. Surface pressures were measured as functions of angle of attack to provide

lift and moment coefficient polars. An actuated wake-rake system was used to examine flow two-dimensionality and to determine drag coefficient.

3.5. Aerodynamic and acoustic results

The main goal of this effort is to compare the noise signature of the serrated trailing edge configurations to the baseline. Integrated spectra and sample acoustic maps for the key configurations and angles of attack have been extracted from the microphone array measurements.

The serrated trailing edge extensions were found to have minimal impact on the airfoil aerodynamics. Pressure distributions on the airfoil and the lift and moment coefficients they imply appear very similar to the baseline airfoil. The largest consistent effect of the serrated extensions is a slight increase in Cl at angles of attack above 8° resulting in a higher maximum lift. In most cases the stall angle remains unchanged.

The drag measurements revealed that the serration tested (a 10%c serration extension configuration) matches the baseline drag levels but that it greatly enhanced the spanwise non-uniformity of the clean airfoil. The addition of a trip strip removed most of the three-dimensionality in the wake producing a closely 2D wake over the center 16% of the airfoil span. This suggests that the spanwise non-uniformity seen on the clean baseline results from spanwise variations in the chordwise location of boundary layer transition.

The results for each serration size (from 5%c to 20%c) have been compared to the baseline and found to produce little to no changes to the lift, suggesting that serration size did not influence the lift of the baseline airfoil within the range of serration parameters investigated. The serration extensions were indeed designed to produce minimal impact on the airfoil lift.

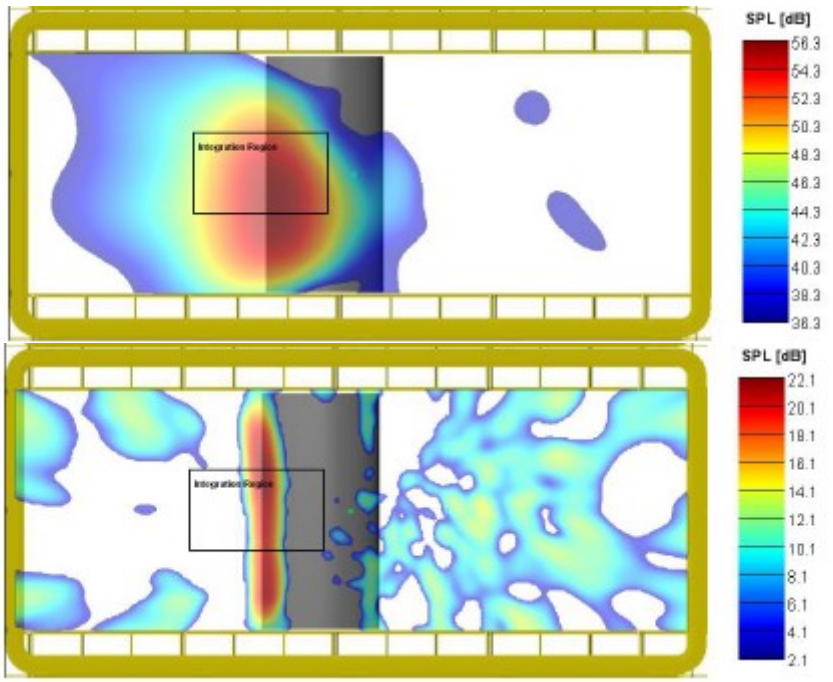

Figure 6: Beamforming map of noise at 1500 Hz (top) and 4750 Hz (bottom)

The beamforming maps show the TBL-TE noise as the dominant noise source, with a very good signal to noise ratio between 1500 Hz to 5000 Hz (figure 7). Below 750 Hz, the TBL-

TE lob merge with tunnel background noise lobs, and it is seen as the low frequency cut-off for integration of sound pressure level.

It was found that all design parameters identified in this study (STE length to chord ratio (h), aspect-ratio (SAR), angle of STE to the chord (ASTE)) govern STE noise reduction effectiveness. Moreover, detailed geometric refinements were added to the design to ensure manufacturability and reduce fatigue issues for 20 years lifetime requirement.

Final results highlight that the best STE design could provide up to 4.5 dBA of noise reduction at low AoA (0 degree) and up to 3.5 dBA noise reductions at operating AoA (5 to 6 degrees). STE affect the noise similarly in clean and tripped boundary layer conditions, giving the same noise reduction.

The following 1/12th octave band spectrum (figure 8) is an integration of the TBL-TE noise, integrated and corrected by the method described in section 3.3. The noise reduction for several serration designs, which are effective in the 500 to 3,000 Hz frequency range in this case, is clearly demonstrated. The peak noise level is well reduced and thus the overall noise level.

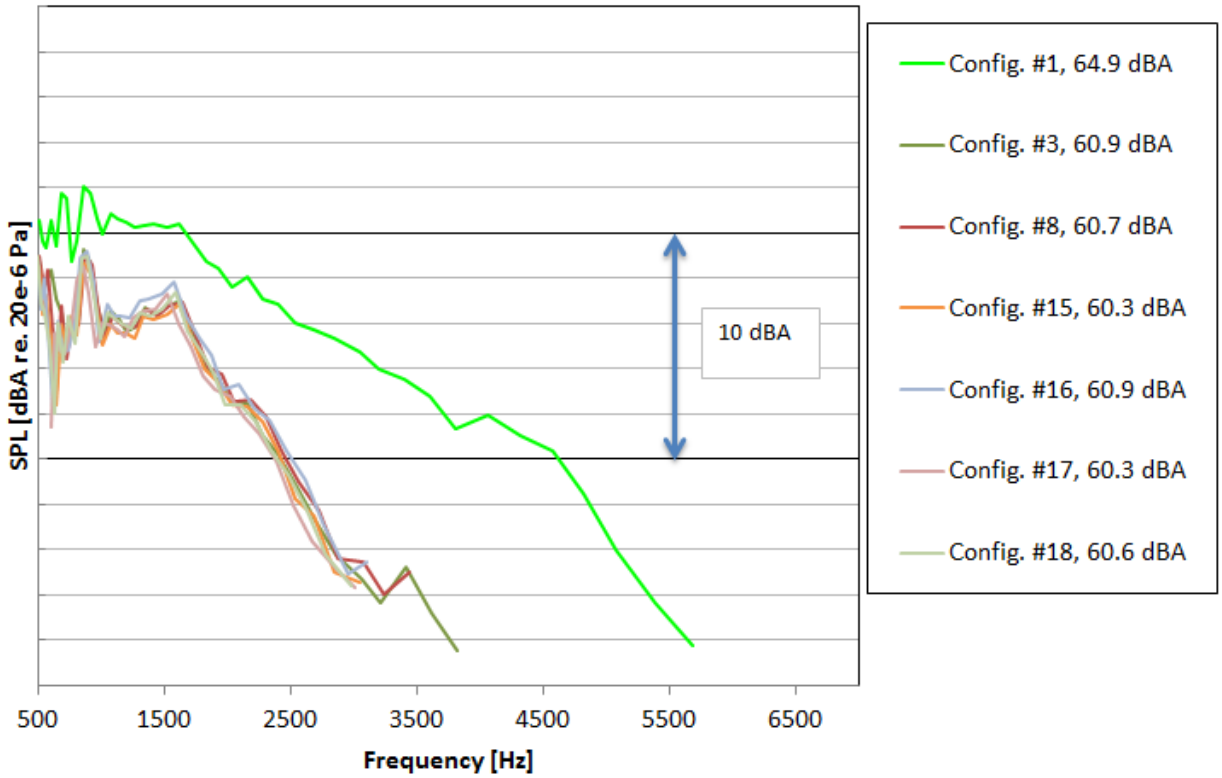

Figure 7: Integrated 1/12th octave spectra of 6 STE configurations compared with the baseline airfoil TBL-TE noise (Config. #1).

4 WTG experimental campaign

4.1 Serration design for rotating blade

Considering the data gathered through the wind tunnel test about the parametric design space of STE, new STE have been designed for a rotating blade. The STE tested in quasi-2D flow (wind tunnel) have been adapted to a 3D flow (rotating blade). Moreover, several STE designs are fitted on one blade to follow the variation of chord and airfoil geometry along the span.

4.2 Noise measurement on V117 at noise mode 0

IEC 61400-11 ed.3 sound power measurement has been performed on the V117 3.3MW wind turbine, with and without STE. V117 is pitch regulated and thus the angle of attack (AoA) will vary significantly with the wind speed. Figure 9 shows that the STE are effective at reducing the overall sound power of the wind turbine on a large wind speed range.

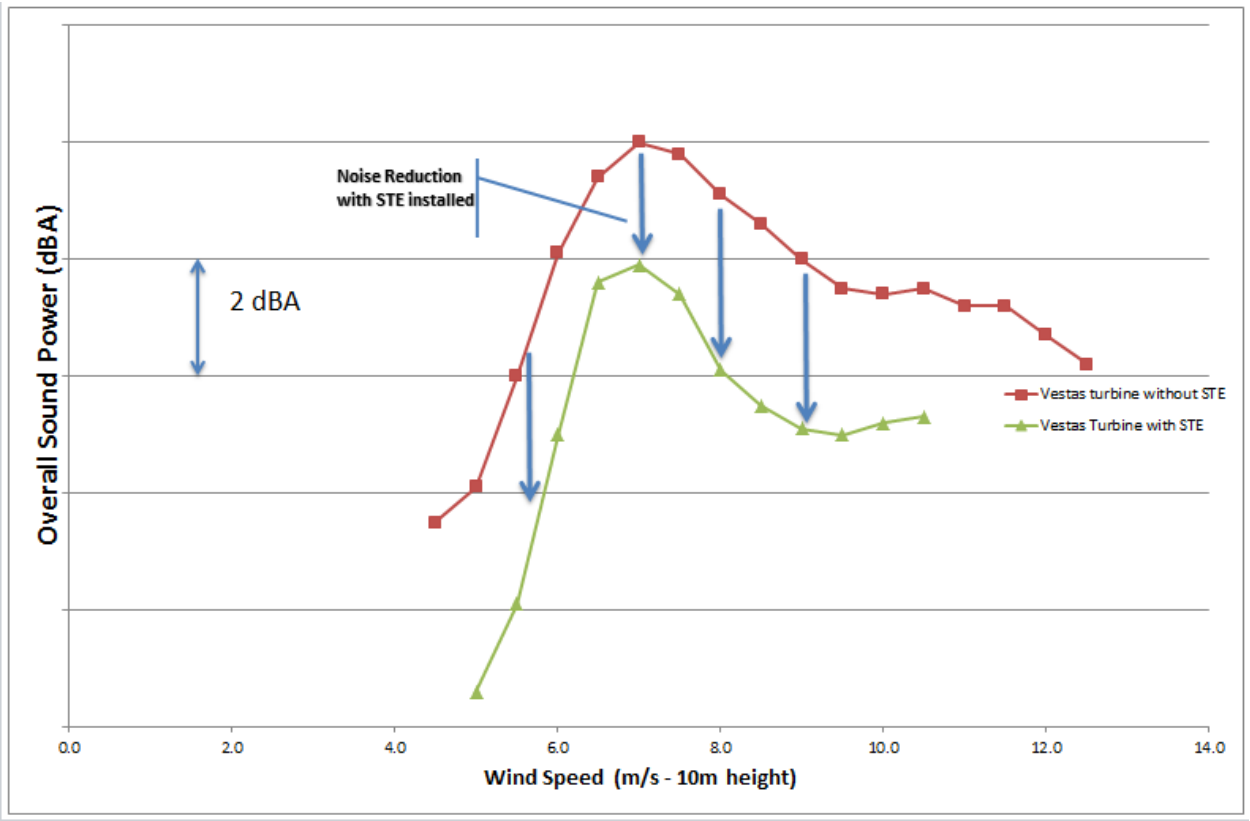

Figure 8: V117 noise curve with and without serration. IEC 61400-11 ed.3 measurement.

The figures are reported in table 1; the overall sound power level reduction is between 1.6 to 3.1 dBA in a large wind speed range of 5-11.5 m/s at 10 m height. The noise reduction is overall very good and in agreement to the wind tunnel measurement. One can expect that the other noise sources generated by the WTG and not tackled by STE would make STE less effective on a full rotor, but these results confirm that TBL-TE noise is the major WTG noise source.

Table 1: Overall sound power level reduction by adding serrations on V117 at noise mode 0.

Bin wind speed at 10m Height [m/s]	Uncertainty of measurement σ	Noise reduction by adding STE (dB)
5	1.31	-2.4
5.5	1.10	-2.4
6	0.90	-1.5
6.5	0.95	-1.6
7	0.85	-1.9
7.5	0.92	-2.3
8	0.99	-2.7
8.5	0.98	-3.1
9	0.98	-3.0
9.5	1.03	-2.7
10	1.04	-2.4
10.5	1.10	-2.2

Figure 10 show a comparison of the 1/3rd octave spectrum with and without serrations, between 100 Hz to 5 kHz. The STE are effective at reducing the sound power level across a wide range of frequencies. The attention to the design of STE, especially for the key parameters, is demonstrated by the absence of high frequency noise increase as it was shown by several authors for other serration designs.

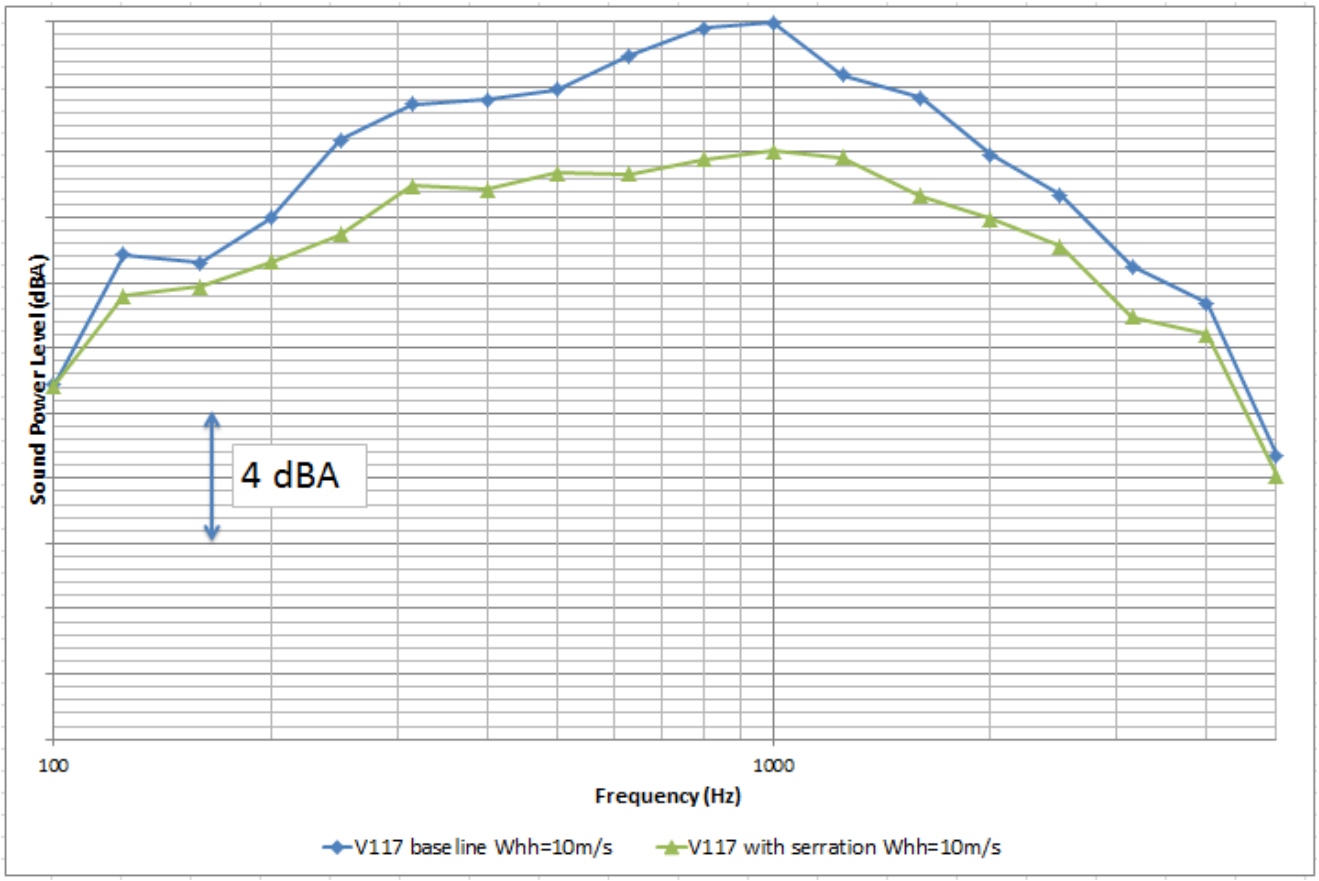

Figure 9: Average 1/3rd octave spectrum at 10 m/s wind speed bin (hub height). Comparison with and without serrations.

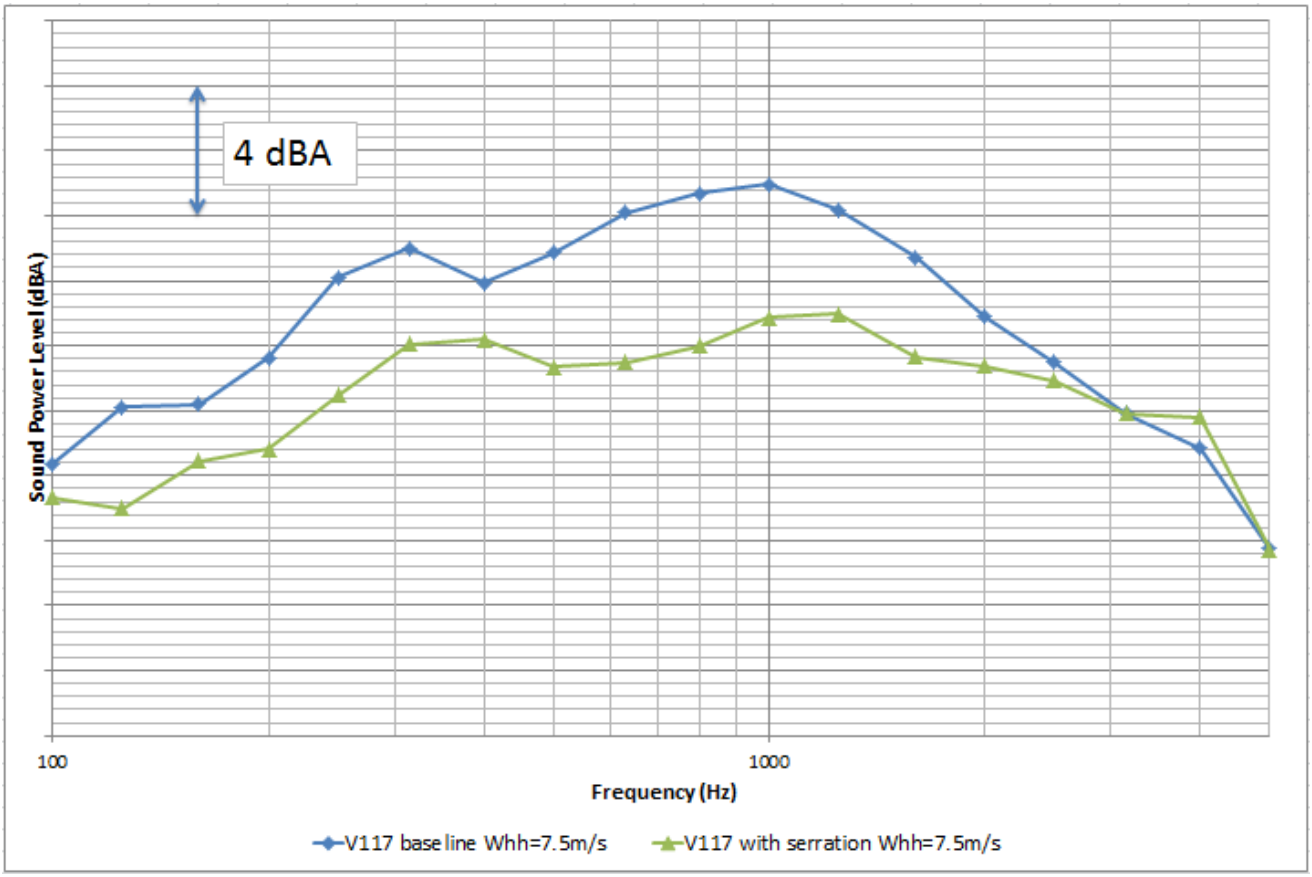

Figure 10: Average 1/3rd octave spectrum at 7.5m/s wind speed bin (hub height). Comparison with and without serrations.

The analysis at other wind speeds, for example 7.5 m/s hub height, confirms the broadband noise reduction on a large frequency range (figure 11).

4.3 Noise measurement for V126 at noise mode 0

In order to assess the robustness of the new STE, it has been applied on a wind turbine of a different wind class. V117 is an IEC2b class wind turbine whereas V126 is an IEC3a. IT is clear on figure 12 that the STE are also very effective for overall noise reduction on V126. The noise reduction varies function of the wind speed bin from 1.6 to 3.5 dBA, as reported on Table 2.

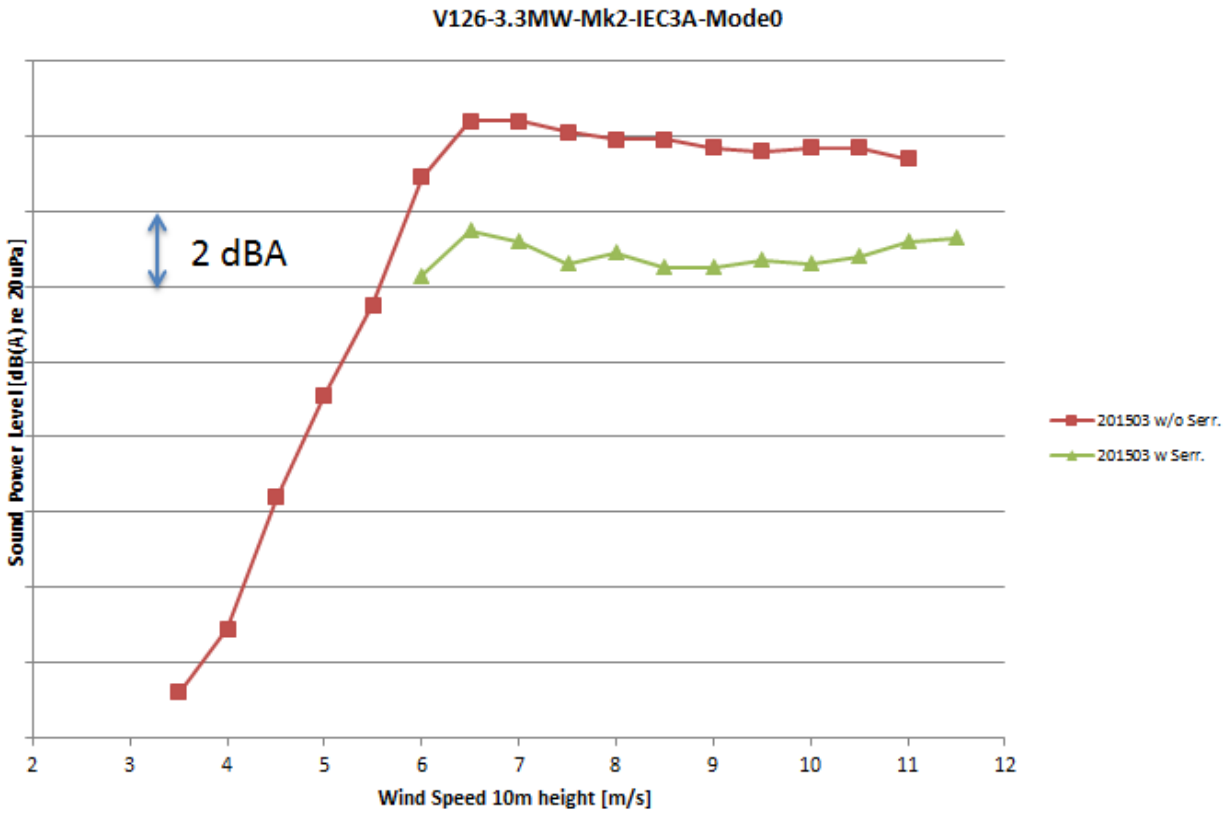

Figure 11: V126 noise curve with and without serration. IEC 61400-11 ed.3 measurement.

Table 2: Overall sound power level reduction by adding serration on V126 at noise mode 0.

Wind speed 10m	Uncertainty	Diff
[m/s]	[dB(A)]	[dB(A)]
6	0.8	-2.6
6.5	0.8	-2.9
7	0.8	-3.2
7.5	0.9	-3.5
8	0.8	-3
8.5	0.9	-3.4
9	0.9	-3.2
9.5	0.9	-2.9
10	1.1	-3.1
10.5	0.9	-2.9
11	0.9	-2.2

4.4 Noise measurement on V117 at noise reduced mode

The following analysis aims at evaluating the STE performance at noise reduced mode. Noise reduced mode allows the WTG to generate less noise by power curtailment. The rotor operates at a lower rotation speed and the pitch setting is tuned for the new rotation speed. Figure 13 represent V117 noise curve at a curtailed noise mode, and the STE are very effective at reducing overall sound power level. All WTG noise modes have been analysed and all show similar noise reduction by addition of STE.

Data are compared in table 3, between 6 to 9.5 m/s wind speed. The noise reduction is between 2.2 to 4.1 dBA, slightly higher than noise mode 0. STE noise reduction is enough to allow WTG operating in noise reduced mode to operate one mode higher (i.e. mode X+1

instead of mode X). This will results in an improved annual energy production by approximately 2-4%, depending on WTG, site and noise mode.

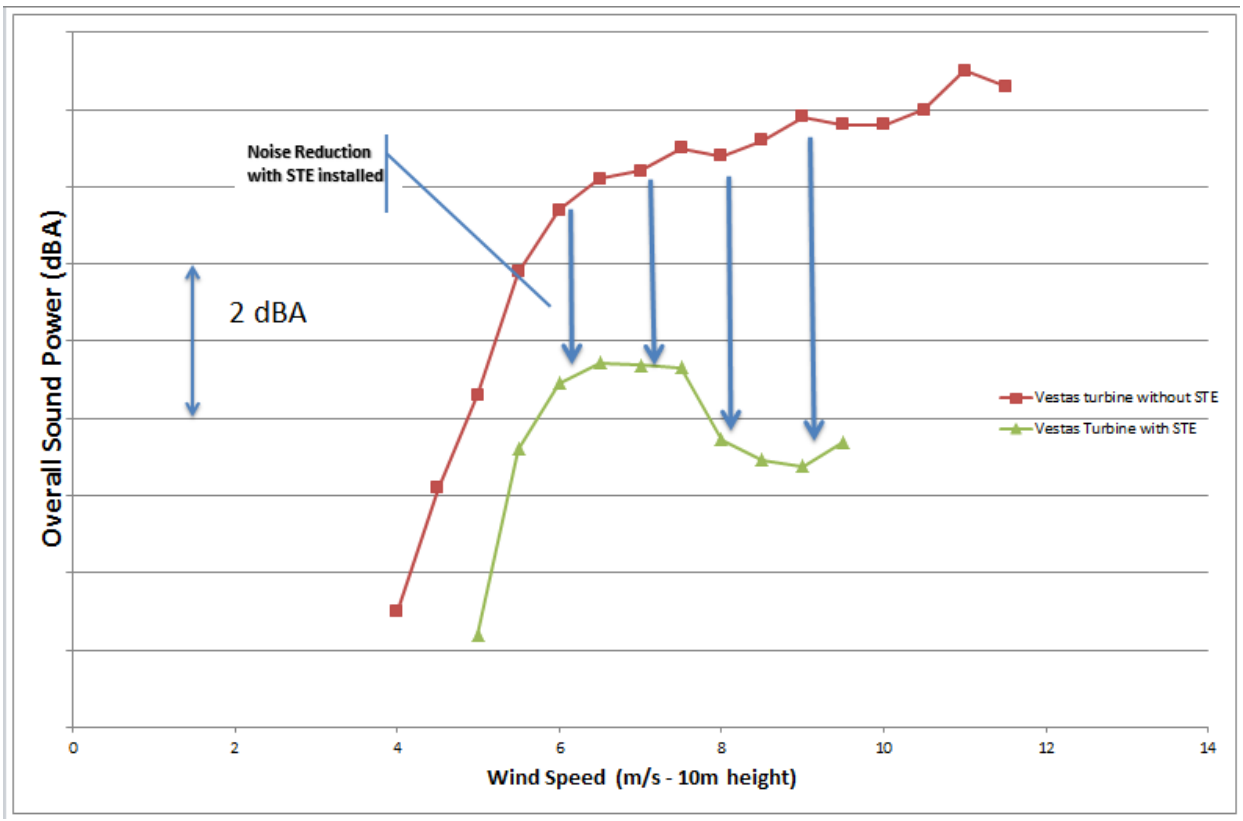

Figure 12: V117 noise curve with and without serration at curtailed noise mode. IEC 61400-11 ed.3 measurement.

Table 3: Overall sound power level reduction by adding serration on V117 at noise curtailed mode.

Bin WS at 10m Height [m/s]	σ	Diff
5	1.4	-3.1
5.5	1.3	-2.3
6	1.1	-2.2
6.5	1.2	-2.4
7	1.2	-2.5
7.5	1.2	-2.8
8	1.5	-3.7
8.5	1.2	-4.1
9	1.3	-4.5
9.5	1.3	-4.1

5 Conclusions

A high fidelity, high Reynolds number wind tunnel experiment has been carried out in order to develop serrated trailing edges for wind turbine noise reduction. The wind tunnel parametric study has been the starting point for STE design for 3D flow and wind turbine rotating blades. The final design is a compromise between noise reduction, aerodynamic loads and serration manufacturability.

The results highlight a very good noise reduction, with 2-3 dBA overall WTG noise reduction, and offers improved competitiveness of VESTAS WTG in noise sensitive markets.

STE provide TBL-TE noise reduction by affecting the scattering efficiency of the edge. Following research could focus on the turbulent boundary layer which is the source of TBL-TE noise. Another passive noise control method that could affect turbulent boundary layer could then be associated with STE for further noise reduction.

6 Acknowledgements

The authors would like to thanks Matt Summers, Eric Schmidt and Jingshu Wu for the design and development of serrations for the 2011/2012 wind tunnel test campaign.

7 References

[1] Howe, M.S., “A Review of the Theory of Trailing Edge Noise”, Journal of Sound and Vibration, 1978, 61(3), 437-465.
[2] Howe, M.S., “Aerodynamic Noise of a Serrated Trailing Edge”, Journal of Fluids and Structures, 1991, 5, 33-45.
[3] Dassen, T., Parchen, R., Bruggeman, J., Hagg, F., ”Results of a Wind Tunnel Study on the Reduction of Airfoil Self-noise by the Application of Serrated Blade Trailing Edges”, National Aerospace Laboratory report, NLR-TP-96350.
[4] Braun, K.A., vd Borg, N.J.C.M., Dassen, A.G.M., Gordner, A., Parchen, R., “Noise Reduction by using Serrated Trailing Edges”, EWEC'97 Proceedings, Dublin, 1997
[5] Dassen, T., Parchen, R., Guidati, G., Wagner, S., Kang, S., Khodak, A.E., ”Comparison of Measured and Predicted Airfoil Self-noise with Application to Wind Turbine Noise Reduction”, National Aerospace Laboratory report, NLR-TP-97564.
[6] Oerlemans, S., Schepers, J.G., Guidati, G., Wagner, S., ”Experimental Demonstration of Wind Turbine Noise Reduction Through Optimized Airfoil Shape and Trailing-Edge Serrations”, National Aerospace Laboratory report, NLR-TP-2001-324.
[7] Oerlemans, S., Fisher, M., Maeder, T., Kogler, K., ”Reduction of Wind Turbine Noise Using Optimized Airfoils and Trailing-Edge Serrations”, National Aerospace Laboratory report, NLR-TP-2009-401.
[8] Sandberg, R.D., Jones, L.E., “Direct Numerical Simulations of Airfoil Self-Noise”, IUTAM Symposium on Computational Aero-Acoustics for Aircraft Noise Prediction, 2010, 6, 274-282.
[9] Herr, M., J. Reichenberger, In Search of Airworthy Trailing-Edge Noise Reduction Means, 17th AIAA/CEAS Aeroacoustics Conference, Portland, USA, AIAA-Paper 2011-2780, 2011.
[10] Gruber, M., Joseph, P.F., Chong, T.P., On the Mechanisms of Serrated Airfoil Trailing Edge Noise, 17th AIAA/CEAS Aeroacoustics Conference, Portland, USA, AIAA-Paper 2011-2781, 2011.
[11] Choi K. and Simpson R.L., 1987, "Some Mean Velocity, Turbulence and Unsteadiness Characteristics of the VPI & SU Stability Wind Tunnel," Department of Aerospace and Ocean Engineering, Virginia Polytechnic Institute and State University, Blacksburg, Virginia 24061, Report VPI-Aero-161.
[12] Jaeger S.M., Horne W.C., and Allen C.S., “Effect of Surface Treatment on Array Microphone Self-Noise,” 6th AIAA/CEAS Aeroacoustics Conference and Exhibit, Lahaina, HI, June 2000. AIAA-2000-1937.
[13] Devenport W.J., Borgoltz A. and Rasnick M., January 2009, “Aerodynamic Measurements To Develop And Validate Porous Wall Wind Tunnel Corrections”, Final report to Sandia under grant 208-11-110F-101-402-1, Department of Aerospace and Ocean Engineering , Virginia Tech.
[14] Mueller T. (ed.), Aeroacoustic Measurements, Springer, 2002. ISBN 3-540-41757-5.
[15] Devenport W.J., Burdisso R.A., Borgoltz A., Ravetta P.A. and Barone M., 2010, “Aerodynamic and Acoustic Corrections for a Kevlar Walled Anechoic Wind Tunnel”, AIAA 16th AIAA/CEAS Aeroacoustics Conference, June 7th-9th 2010, Stockholm, Sweden. AIAA Paper 2010-3749.
[16] Ffowcs Williams, J.E., Hall, L.H. “Aerodynamic sound generation by turbulent flow in the vicinity of a scattering half plane”, Journal of Fluids Mechanics, 1970, vol. 40, part 4, pp. 657-670.